BEST AVAILABLE IMAGES

Defective images within this document are accurate representations of the original documents submitted by the applicant.

Defects in the images may include (but are not limited to):

- BLACK BORDERS
- TEXT CUT OFF AT TOP, BOTTOM OR SIDES
- FADED TEXT
- ILLEGIBLE TEXT
- SKEWED/SLANTED IMAGES
- COLORED PHOTOS
- BLACK OR VERY BLACK AND WHITE DARK PHOTOS
- GRAY SCALE DOCUMENTS

IMAGES ARE BEST AVAILABLE COPY.

As rescanning documents *will not* correct images, please do not report the images to the Image Problem Mailbox.

APPENDIX
COMPLETE COPY OF UDD (KIM) ARTICLE

[21] Noda, J., Okamoto, K., and Sasaki, Y. (1986) *J. Lightw. Techn.* 4, 1071.
[22] Pavlath, G. A., and Shaw, H. J. (1982). *Appl. Opt.* 21, 1752.
[23] Post, E. J. (1972). *J. Opt. Soc. Am.* 62, 234.
[24] Ulrich, R. (1980). *Opt. Lett.* 5, 173.
[25] Ezekiel, S. (1982). In *Fiber-Optic Rotation Sensors*, S. Ezekiel and H. J. Arditty, eds., p. 2, Springer-Verlag, Berlin, Heidelberg, New York.
[26] Ulrich, R. (1982). In *Fiber-Optic Rotation Sensors*, S. Ezekiel and H. J. Arditty, eds., p. 52, Springer-Verlag, Berlin, Heidelberg, New York.
[27] Cahill, R. F., and Udd, E. (1979). *Opt. Lett.* 4, 93.
[28] Giallorenzi, T. G., Bucaro, J. A., Dandridge, A., Sigel, G. H., Cole, J. H., Rashleigh, S. C., and Priest, R. G. (1982). *IEEE J. Quant. Electronics* QE-18, 626.
[29] *Handbook of Mathematical Functions*, M. Abramovitz and I. A. Stegun, eds., (1964). U.S. Department of Commerce, Washington, D.C.
[30] Wang, C. S., Cheng, W. H., Hwang, C. J., Burns, W. K., and Moeller, R. P. (1982). *Appl. Phys. Lett.* 41, 587.
[31] Burns, W. K., Duling, I. N., Goldberg, L., Moeller, R. P., Villaruel, C. A., Snitzer, E., and Po, H. (1989). *Proc. Conf. on Optical Fiber Sensors OFS'89*, Paris, p. 137.
[32] Trommer, G. F., Poisel, H., Buehler, W., Hartl, E., and Muller, R. (1990). *Appl. Opt.* 29, 5360.
[33] Lyot, B. (1928). *Ann. Obs. Astron. Phys.* [Paris] 8, 102.
[34] Burns, W. K. (1983). *J. Lightwave Techn.* LT-1, 475.
[35] Chien, P. Y., and Pan, C. L. (1991). *Opt. Lett.* 16, 189.
[36] Kintner, E. C., (1981). *Opt. Lett.* 63, 154.
[37] Burns, W. K., and Moeller, R. P. (1984). *J. Lightwave Techn.* LT-2, 430.
[38] Burns, W. K., and Moeller, R. P. (1985). *J. Lightwave Techn.* LT-3, 209.
[39] Fredericks, R. J., and Ulrich, R. (1984). *El. Lett.* 20, 330.
[40] Burns, W. K. (1986). *J. Lightwave Techn.* LT-4, 8.

Chapter 3

SIGNAL PROCESSING TECHNIQUES

B. Y. Kim

Department of Physics
Korea Advanced Institute of Science and Technology
Taejon

1. INTRODUCTION

As described in previous chapters, the basic output intensity response of the Sagnac interferometer to rotation rate is nonlinear and periodic, making it necessary to incorporate optical or electronic signal processing in order to achieve the desired sensitivity and dynamic range. The origin of this problem lies in the fact that the rotation-induced phase shift (Sagnac phase shift), which is linearly proportional to the rotation rate, is converted into a change in the intensity of the optical output from the interferometer. This problem is common to the basic response of all optical interferometers since only the intensity of light can be measured directly with existing square law photodetectors. In other words, one would not have

ISBN 0-12-146075-4

had the nonlinear response problem if a photodetector existed that could directly monitor the phase of an optical signal. This chapter describes several signal processing techniques to convert the basically nonlinear response of the gyroscope to a linear one.

The basic response of a gyro in terms of output intensity or detector current is proportional to $[1 + \cos(\phi_R)]$ as shown in Figure 3.1, where $\phi_R = 2\pi LD\Omega/\lambda c$ is the Sagnac phase shift. We can see from this curve that (i) the sensitivity of output to rotation rate is zero whenever the Sagnac phase shift is $N\pi$ (N: integer) including zero rotation rate; (ii) when starting from $\phi = N\pi$, there is no way of telling the direction of rotation due to the symmetry of the response curve, (iii) due to the periodic nature of the response curve, there is an ambiguity of $2N\pi$ in the measurement ϕ especially when the gyro is initiated while it is rotating at a high speed. The main concern of this chapter is with solutions for problems (i) and (ii). The solution for the problem (iii) requires additional information from the gyroscope, which complicates the optical circuit, such as by using two optical sources with different wavelengths for wavelength multiplexing. This particular problem is not considered to be serious for gyro applications, where the gyro can always be initiated at zero rotation rate.

The problems of limited dynamic range and sensitivity just mentioned could be solved by forcing the response of the gyro output to be monotonic (preferably linear) with the rotation rate. Generally speaking, there are two different approaches to linearizing the gyro response; namely, the closed-loop and open-loop approaches. For the closed-loop approach, an electronic–optical control element, added to the sensing loop of the gyro, introduces a nonreciprocal phase difference between the counterpropagating optical waves ($\Delta\phi$) in response to the rotation input and compensates for the rotation-induced Sagnac phase shift (see Figure 3.2). In this manner, the total phase difference between the interfering optical waves is kept constant (such that $\Delta\phi_{NR} + \phi_R = 0$) at all times regardless of the

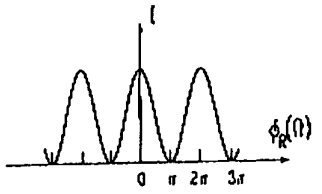

Fig. 3.1. Basic response of a gyro output intensity or a detector current with respect to Sagnac phase shift.

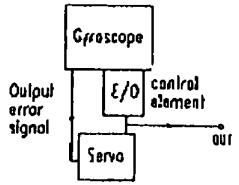

Fig. 3.2. The functional schematic of a closed-loop gyroscope.

rotation rate, and the amount of nonreciprocal phase difference introduced to achieve such a condition is measured as the output of the gyroscope. The detector output of a closed-loop gyro is used as an error signal for the feedback servo loop. Since the Sagnac phase shift, which is linearly proportional to the rotation rate, is measured as the output, the response of a closed-loop gyro is basically linear in the rotation rate. One of the principal advantages of closed-loop gyroscopes is that the rotation signal output is independent of the optical intensity and the gain factor of the detection electronics, when the error signal is kept at zero (with the dynamic biasing described in the following section). The major difficulty with the closed-loop approach lies in finding a proper electronic–optical element that can effectively produce a nonreciprocal phase shift in a stable and controlled manner, since the fiber gyro is carefully designed to guarantee the two interfering waves travel exactly the same optical paths. For this purpose, optical frequency shifters and phase modulators are commonly used. These control elements are reciprocal devices, but they are placed at an asymmetric position in the gyro sensing loop so that the two counterpropagating waves pass through the device at different times before they interfere with each other. When the device is located at one end of the gyro sensing loop, the time difference corresponds to the flight time, τ, of light through the fiber length in the sensing loop. A frequency shifter located near one end of a gyro sensing loop creates a difference in the frequencies of counterpropagating optical waves in the sensing loop, Δf, that results in an accumulated phase difference of $\Delta\phi = 2\pi\Delta f\tau$, which can be accurately controlled by the magnitude of the frequency shift Δf. The role of a frequency shifter in a gyroscope is identical to that of a phase modulator producing a linear phase ramp with respect to time. A time-varying phase modulator located at one end of the gyro sensing loop produces a time-varying phase difference between the two counterpropagating optical waves with a time averaged phase shift of zero, in contrast to frequency shifters, since a practical phase modulator cannot generate an infinitely increasing phase ramp without resetting the magnitude of the

phase shift. A number of approaches using periodic phase modulation waveforms and electronic gating of the detector output have been introduced to get around this problem, which will be discussed in detail in this chapter.

Open-loop approaches to linear response of gyroscopes do not involve a nonreciprocal phase shifter (see Figure 3.3) leading to a simpler optical arrangement. Their electronic signal processing to get a linear response tends not to be straightforward. The fundamental principle of open-loop approaches is to use the gyro detector output, which has both sine and cosine functions of the Sagnac phase shift, from which the rotation-induced phase shift is obtained either by analog or digital electronic signal processing. Since the Sagnac phase shift is linear in the rotation rate, the final output from an open-loop gyro is linearly proportional to the rotation rate, solving the sensitivity and dynamic range problems. As in the case of closed-loop gyros, the output of an open-loop gyro can be independent of optical power and electronic gain factors when the preceding quadrature phase information is used. Since the basic output of a fiber gyroscope has $[1 + \cos(\phi_R)]$ dependence on the Sagnac phase shift, special methods need to be incorporated to produce a $\sin(\phi_R)$ dependant signal in addition to the $\cos(\phi_R)$ term. A commonly used technique is the application of a time-varying phase difference modulation to the counterpropagating optical waves so that the operation point of the gyro never stays at a single point on the response curve shown in Figure 3.1. In very general terms, the gyro output waveform with a time-varying phase modulation contains information as to where on the cosine curve the center of the phase modulation is located from which the Sagnac phase shift (that is normally slowly varying compared to the applied phase modulation) can be measured. The major issue with the open-loop approaches is the performance of electronic signal processing, since it should satisfy the sensitivity and dynamic range requirements of the gyroscopes.

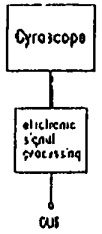

Fig. 3.3. The functional schematic of an open-loop gyroscope.

2. PHASE MODULATION IN GYROSCOPES

In an ideal fiber gyroscope with reciprocal configuration, as shown in Figure 3.4, the counterpropagating optical waves that reach the photodetector are designed to travel exactly the same optical paths so that the rotation-induced Sagnac phase shift is the only source of nonreciprocal phase shift. For this reason, it is not straightforward to introduce a controlled amount of nonreciprocal phase shift with a nonzero time-averaged value. However, it is relatively easy to generate a time-varying phase modulation with a zero phase offset in the following way. Suppose a phase modulator is located at an asymmetric position in the sensing loop of a gyroscope with respect to the center of the fiber loop or the directional coupler that forms the sensing loop as shown in Figure 3.5. When a modulation signal $\phi(t)$ is produced by the phase modulator, the modulation in the phase difference between the counterpropagation waves $\Delta\phi(t)$ becomes

$$\Delta\phi(t) = \phi_{ccw}(t) - \phi_{cw}(t) = \phi(t) - \phi(t - \tau) \qquad (3.1)$$

where ϕ_{ccw} and ϕ_{cw} represent the phases of optical waves that propagate in counterclockwise and clockwise directions in the sensing loop, and τ is the transit time of light between the phase modulator and its symmetric position in the loop. It can be seen from equation (3.1) that the gyroscope differentiates an applied phase modulation when the modulation period is slow compared to τ, leading to the immunity of the fiber gyro to external phase perturbation noise. A further suppression of the effects of time-varying phase perturbation is achieved by arranging for symmetric positions along the fiber to be close to each other in a multiturn fiber coil. When phase modulation is desired in the fiber gyro, a phase modulator is placed at one end of the sensing fiber loop near the directional coupler, in which case τ becomes the transit time of light through the entire fiber length in the sensing loop (called *loop transit time* $\tau = nL/c$, where n is the effective

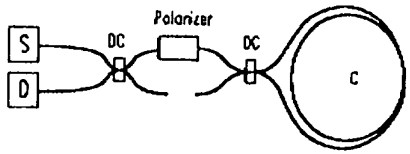

Fig. 3.4. The minimum configuration for a reciprocal gyroscope. *S*: source, *D*: detector, *DC*: directional coupler, *C*: sensing coil.

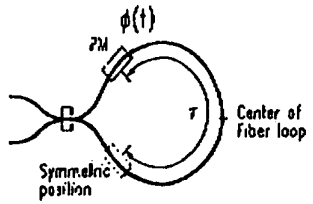

Fig. 3.5. A gyro sensing loop with a phase modulator (*PM*) located near one end of the loop.

group refractive index of the fiber, L is the length of the fiber loop, and c is the speed of light in vacuum). For a sinusoidal phase modulation $\phi(t) = \phi_0 \sin(\omega t)$,

$$\Delta\phi(t) = 2\phi_0 \sin(\omega\tau/2)\cos\{\omega(t - \tau/2)\} \tag{3.2}$$

As can be seen from this equation, the maximum phase difference modulation for a given ϕ_0 can be achieved when $\omega = \pi/\tau$, which is often called the *characteristic frequency* or *proper frequency* for phase modulation. Figure 3.6 shows the waveforms of $\Delta\phi(t)$ for various periodic waveforms of $\phi(t)$ with fundamental frequency ω, for $\omega < \pi/\tau$ and $\omega = \pi/\tau$. Arbitrary waveforms of $\Delta\phi(t)$, including the examples shown in this figure, can be generated with wideband electro-optic phase modulators such as those using $LiNbO_3$ channel waveguide. The most commonly used fiber optic phase modulator, which is a section of fiber wound around a piezoelectric cylinder, is inherently a narrowband device limited in practice to the generation of sinusoidal phase modulation waveforms.

When a sinusoidal phase difference modulation $\Delta\phi(t) = \phi_m \sin(\omega_m t)$ is applied to a gyroscope, the detector current $I_d(t)$, which is proportional to the optical intensity, is

$$\begin{aligned} I_d(t) &= I_0/2[1 + \cos(\phi_m \sin\omega_m t + \phi_R)] \\ &= I_0/2\Big[1 + \{J_0(\phi_m) + 2\textstyle\sum J_{2n}(\phi_m)\cos(2n\omega_m t)\}\cos(\phi_R) \\ &\quad - 2\textstyle\sum J_{2n-1}(\phi_m)\sin\{(2n-1)\omega_m t\}\sin(\phi_R)\Big] \end{aligned} \tag{3.3}$$

where I_0 is the peak detector current and J_n denotes the nth order Bessel function of the first kind. It can be seen from equation (3.3) that signals with both the sine and cosine dependence on Sagnac phase shift (ϕ_R) can be readily available at odd and even harmonics of the differential phase modulation frequency $\omega_m (= 2\pi f_m)$, respectively, whereas the output signal from a gyro without a phase modulation is proportional to $[1 + \cos(\phi_R)]$ with only the cosine dependence. As discussed in Section 1, one has all the necessary information to calculate ϕ_R, which is linearly proportional to rotation rate, in the detector current from a phase-modulated gyroscope. For example,

$$\phi_R = \tan^{-1}\{I(\omega_m)J_2(\phi_m)/I(2\omega_m)J_1(\phi_m)\} \tag{3.4}$$

where $I(\omega_m)$ and $I(2\omega_m)$ are the amplitudes of detector current at the first and second harmonics of the phase modulation frequency. Although this straightforward calculation is not the best way to obtain the value of ϕ_R, and thus the rotation rate, it shows the basic idea of getting a linear response of the gyro with rotation rate for open-loop gyroscopes, which will be discussed in more detail in Section 4. Another important aspect of

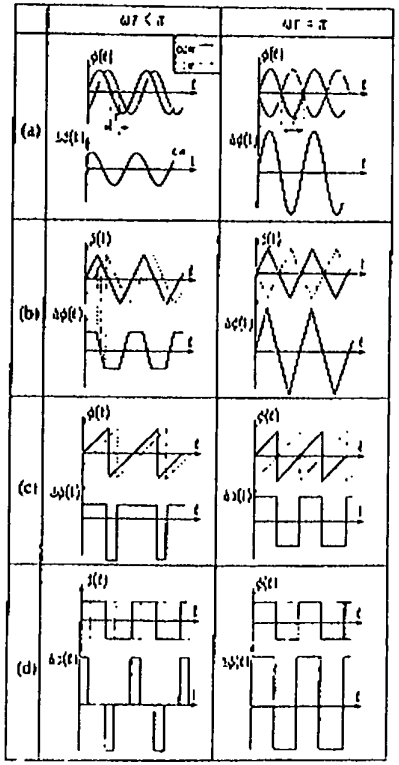

Fig. 3.6. Differential phase modulation waveforms $\Delta\phi(t)$ for several periodic phase modulation waveforms $\phi(t)$ and for two values of $\omega\tau$.

the output from a phase modulated gyroscope (equation (3.3)) is that the odd harmonic components of the detector current are proportional to $\sin(\phi_R)$, leading to a maximum sensitivity near zero rotation rate ($\phi_R \ll 1$) when one of the odd harmonic components of the detector current is measured as the output of the gyroscope [1–3]. Typically the amplitude of the first harmonic signal $I(\omega_m)$ is measured with a lock-in amplifier, and the amplitude of the differential phase modulation, ϕ_m, is adjusted to be 1.84 rad where $J_1(\phi_m)$ is maximum. Figure 3.7 shows $I(\omega_m)$ as a function of ϕ_R. However, the linear dynamic range of the gyro is still limited to less than the rotation rate corresponding to a Sagnac phase shift of $\pi/2$ in either direction of rotation. This situation is equivalent to biasing the operating point of a gyroscope to the maximum slope point on the basic gyro response curve in Figure 3.1, with an equivalent phase offset of $\pi/2$. A more accurate description is that the gyro operating point is being switched between approximately $+\pi/2$ and $-\pi/2$ of differential phase shift with 50% duty cycle. For this reason this technique of biasing the gyro signal to the sensitive point near zero rotation rate is often called *dynamic biasing*. This way of understanding the dynamic biasing becomes more clear if the sinusoidal waveform of the differential phase modulation is replaced by a square waveform with amplitude of $\pi/2$ (see Figure 3.8). Some fiber gyros actually use the square waveform instead of a sinusoidal one for dynamic biasing. The fact that the operating point of a dynamically biased gyroscope spends an equal amount of time on the positive and negative slopes of the response curve, in a symmetric fashion, is important since it makes the gyroscope reciprocal in a time averaged fashion. The significance of this point becomes clear when compared to a gyro with a "static" bias on one side only (say, $\pi/2$), where it becomes very difficult to stabilize the magnitude of the large nonreciprocal phase shift within the extremely small Sagnac phase shift (on the order of 10^{-7} rad) one wants to measure. All of the closed-loop gyroscopes use dynamic biasing in order to get a sensitive measurement of deviation of Sagnac phase shift from zero

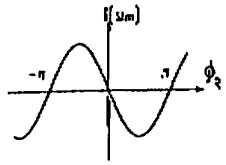

Fig. 3.7. The amplitude of detector current at the phase modulation frequency ω_m as a function of the Sagnac phase shift ϕ_R.

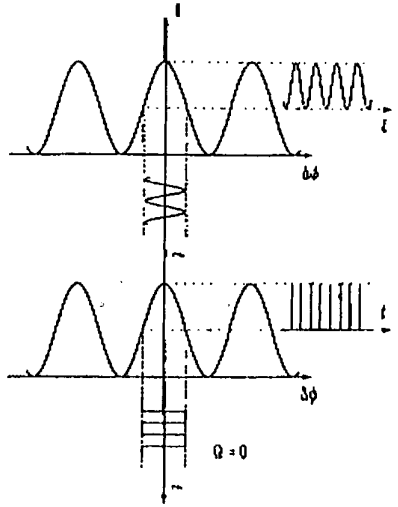

Fig. 3.8. Dynamic biasing of the gyroscope with sinusoidal and square waveforms

and maintain the net phase shift (Sagnac phase shift plus added nonreciprocal phase shift by a nonreciprocal phase shifter) at zero.

3. CLOSED-LOOP APPROACHES

As mentioned in Section 1, the key to the closed-loop operation of gyroscopes is to devise a proper way of introducing a controlled amount of nonreciprocal phase shift between the counterpropagating optical waves in the sensing fiber loop. Another important aspect of closed-loop gyroscopes is that they all utilize the dynamic bias, which involves a phase modulation as described in the previous section and phase sensitive demodulation using a lock-in detection of the first harmonic of the applied phase modulation frequency. The division of different closed-loop approaches is made depending on the methods used to produce the nonreciprocal phase shift. At the early stage of fiber-optic gyroscope development, acousto-optic frequency shifters located at one end of the sensing fiber loop were used for this purpose. Later, phase modulators were used in a number of different ways to generate a nonreciprocal phase shift.

All the nonreciprocal phase shifters used in a closed-loop fiber gyroscopes are in fact reciprocal components incorporated in the gyroscope in such a way that they produce differential phase shift between the counter-

propagating waves similar to the phase modulator described in Section 2. The fundamental operating principle of the so-called nonreciprocal phase shifters relies on the time difference for the counterpropagating waves to pass through an optical element that generates time-varying optical phase change, leading to a differential phase shift. The phase shifter used for this purpose is always located at one end of the sensing loop, and the time difference involved is $\tau = nL/c$, where L is the length of fiber loop.

An ideal form of the phase modulation for producing a constant phase difference between the counterpropagating waves is a continuous phase ramp in time, as shown in Figure 3.9. In this case with $\phi(t) = \alpha t$, the differential phase shift expressed in equation (3.1) is $\Delta\phi(t) = \alpha\tau$, which is constant in time. Therefore, by varying the slope of the phase ramp, α, the amount of differential phase shift can be controlled and used to counteract the rotation induced phase shift and maintain the net differential phase shift of the gyroscope at zero. The only optical components currently used to produce an infinite phase ramp are acousto-optic frequency shifters with $\phi(t) = \Delta\omega t$, where $\Delta\omega$ is the amount of frequency shift applied to the optical wave. Other forms of phase modulators, such as fiber-optic and integrated-optic phase modulators, cannot produce an infinite phase ramp, since they would require infinitely increasing strain in a fiber or infinitely increasing voltage applied to an electro-optic modulator.

To avoid this problem and still simulate the effect of an infinite phase ramp, a so-called serrodyne phase modulation waveform is used as shown in Figure 3.10. The serrodyne phase modulation is essentially a phase ramp with periodic reset with amplitude ϕ_m and period T, and the differential

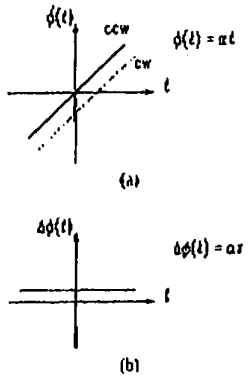

Fig. 3.9. (a) A continuous phase ramp $\phi(t) = \alpha t$ generates (b) a constant differential phase $\alpha\tau$.

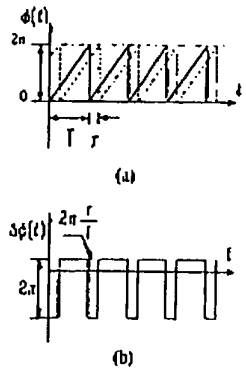

Fig. 3.10. (a) A serrodyne phase modulation waveform, and (b) the corresponding differential phase modulation.

phase shift $\Delta\phi(t)$ is similar to that of an infinite phase ramp except for a time period τ for every cycle of the sawtooth waveform near the resetting time. During the $T - \tau$ time period, the induced differential phase shift $\Delta\phi(t) = \phi_m\tau/T$, which can be adjusted by controlling either the period T (or the frequency $f = 1/T$) or the modulation amplitude ϕ_m. If $\phi_m = 2\pi$, the phase shift during the time period τ differs from that of time period $T - \tau$ by 2π. In this case, the full waveform of $\Delta\phi(t)$ can be used to null the effect of rotation induced phase shift due to the periodic response of the interferometer with 2π periodicity in phase difference as shown in Figure 3.11, where the gyro operating point jumps between $\Delta\phi = 0$ and $\Delta\phi = 2\pi$. The slope of the phase ramp is controlled by adjusting the frequency of the sawtooth waveform that becomes the output of the closed-loop gyroscope as in the case of the frequency shifter.

The nature of the outputs from these two approaches are basically the same. When the amplitude ϕ_m is used to control the slope of the phase ramp with fixed frequency of the sawtooth modulation waveform, only a portion of the waveform $\Delta\phi(t)$, i.e., either $T - \tau$ or τ time period, can be used to counteract the rotation induced phase shift. Therefore, an electronic switching of the detector current must be used to select the signal during the proper time period. The output of this gyroscope is the amplitude of the phase modulation waveform, which is generally not straightforward to measure with high accuracy and large dynamic range. This approach is called the *gated phase modulation approach*. Other phase modulation waveforms that provide a relatively flat differential phase shift $\Delta\phi(t)$ during a fractional period of phase modulation (see Figure 3.6) can

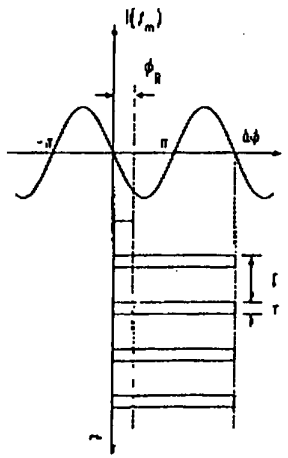

Fig. 3.11. Compensation of rotation induced Sagnac phase shift ϕ_R by using a differential phase modulation like that depicted in Figure 3.10(b).

be used to operate a closed-loop gyroscope with an electronic gate. Some waveforms provide a greater duty cycle than others, and various forms of closed-loop gyros have been demonstrated using the principles just described. In the following, different implementations of nonreciprocal phase shifters for the closed-loop operation of fiber gyroscopes are discussed.

3.1. Frequency Shifter

A conventional acousto-optic frequency shifter (Bragg cell) is a reciprocal device in the sense that the waves propagating in opposite directions along the same path experience the same frequency shift. When a frequency shifter is placed at one end of the sensing loop of a gyroscope as shown in Figure 3.12, the optical waves exiting the loop after propagating through the loop in clockwise (cw) and counterclockwise (ccw) directions have the same optical frequency that is shifted by $\Delta\omega$ from the input optical

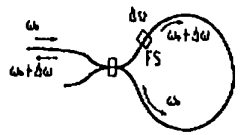

Fig. 3.12. A gyro sensing loop with a frequency shifters (*FS*) located at one end of the loop.

frequency ω_0. However, a differential phase shift is introduced between the counterpropagating waves due to their frequency difference $\Delta\omega$ while they are traveling through the loop, and the magnitude of the phase difference becomes $\Delta\phi = \Delta\omega\tau$, where τ is the transit time of light through the fiber sensing loop. In the case of closed-loop operation with rotation input to the gyroscope, the total differential phase shift is maintained at $\Delta\phi = \phi_R + \Delta\omega\tau = 0$, which leads to an output frequency shift $\Delta f = \Delta\omega/2\pi$ of

$$\Delta f = (D/n\lambda)\Omega \tag{3.5}$$

Compared to the basic response of an open-loop gyroscope, the output of this gyroscope has a linear response to rotation rate with frequency output, and the scale factor depends only on the diameter of the sensing loop, D, source wavelength, λ, and the refractive index n of the fiber. This is basically the same scale factor one finds in active ring laser gyroscopes. The scale factor does not depend on the optical intensity and electronic gain parameters, leading to an improved stability of the scale factor. However, the newly introduced dependence on the refractive index of the fiber causes an instability of the scale factor especially for a relatively high rotation rate, since the refractive index change of a silica glass is 10^{-5}/°C. Methods of monitoring changes in the propagation time of light through the fiber sensing coil, τ, due to the change in the refractive index or the fiber length, have been demonstrated by switching the frequency shift between different values.

An important consideration for any closed-loop approach is that a large static phase bias should be avoided so that the reciprocity of the gyroscope is preserved to prevent any instability of the phase bias. This requires the frequency shifter used in the closed-loop gyroscope to be operated with a center frequency of zero and with a broad enough frequency tuning range to cover the required dynamic range of the gyroscope. As an example, for a 10 cm sensing coil with 1 μm optical wavelength to cover the rotation rate of 10^{-2} to 10^{6}°/h, Δf should cover from 3 mHz to 300 KHz. Unfortunately, conventional Bragg cells operate with a high center frequency of a few tens to a few hundreds of MHz, introducing an untolerable phase bias between the two counterpropagating waves. This forces one to use two frequency shifters with the same center frequency located at symmetric positions in the sensing loop as shown in Figure 3.13 [4, 5]. At zero rotation rate, the two frequency shifters operate at the same frequency f_1 resulting in reciprocal operation of the gyroscope. With rotation inputs, one of the frequency shifters, FS2, adjusts its frequency by Δf in

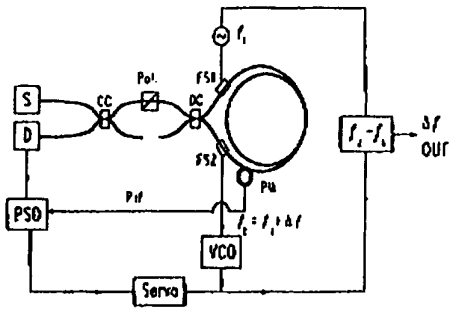

Fig. 3.13. Schematic of a closed-loop gyro with two frequency shifters. *S*: source; *D*: detector; *PSD*: phase sensitive demodulator; *VCO*: voltage controlled oscillator, *FS1*, *FS2*: frequency shifters; *DC*: directional coupler; *PM*: phase modulator.

order to maintain the net differential phase shift at zero, and the rotation rate output is measured as in equation (3.5). Since the readout is in the form of the frequency of an electronic signal that can be measured with high accuracy and conventional equipment, no further electronic signal processing is required with this approach.

Different types of acousto-optic frequency shifters have been used for closed-loop gyroscopes, including two conventional bulk-optic Bragg cells located at each end of the sensing loop or a cleverly designed baseband Bragg cell with center frequency of zero [6] located at one end of the sensing loop. For the latter case, the Bragg cell has two separate acoustic transducers attached to a single acoustic cell, operating at frequencies f_1 and $(-f_1 + \Delta f)$, so that the light passing through the device experiences a net frequency shift of Δf. This not only simplifies the optical circuit but also eliminates the possible bias due to the difference in the distance of the two Bragg cells from the loop directional coupler. The bulk optic Bragg cells are difficult to implement in the single-mode fiber circuit since they require a great deal of alignment accuracy and also mechanical stability in the fiber pigtail. In order to solve this problem, all fiber versions of acousto-optic frequency shifters have been developed using birefringent single-mode fibers or elliptical core two-mode fibers [7]. The latter, shown in Figure 3.14 demonstrated full optical power conversion efficiency with low input electrical power. One of the requirements for the frequency shifter for use in the gyroscope is high spectral purity, expressed as the carrier to sideband extinction ratio. In order to avoid spurious error terms in the gyro output due to the existence of unwanted optical frequency components, the shifted frequency component should have its

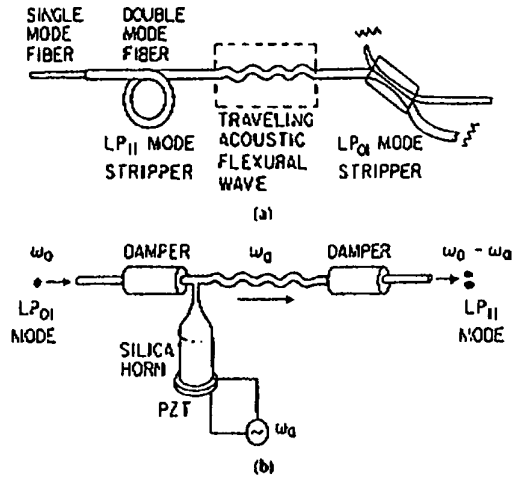

Fig. 3.14. All-fiber-optic frequency shifter using two-mode fiber and acoustic flexural wave.

intensity greater than that of other frequency components by more than 60 dB for less than a few microradians of phase error in the gyroscope. Both commercial bulk-optic frequency shifters and fiber-optic frequency shifters approach the performance required for most applications.

3.2. Analog Serrodyne Phase Modulation

The most straightforward phase modulation waveform to introduce a differential phase shift between the two counterpropagating waves is the sawtooth waveform that simulates a continuous phase ramp, as described previously [8, 9]. The general configuration of the gyroscope using a serrodyne phase modulation is shown in Figure 3.15. The phase modulator located at one end of the sensing loop provides a dynamic biasing as described in Section 2 and also serves as a nonreciprocal phase shifter in the gyroscope. The detector current at the dynamic bias frequency is monitored using a phase sensitive detector (or lock-in amplifier), and the servo loop adjusts the frequency or amplitude of the phase modulation in order to maintain the PSD output at zero. In this case the amount of differential phase shift measured in the form of the frequency or the amplitude of phase modulation applied to the phase modulator represents the rotation induced Sagnac phase shift.

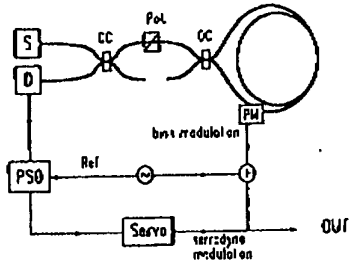

Fig. 3.15. Schematic of a closed-loop gyro with serrodyne phase modulation. *S*: source, *D*: detector, *DC*: directional coupler, *PSD*: phase sensitive demodulator.

The choice of phase modulation waveform depends on the bandwidth of the phase modulator itself and electronic and optical parameters of the gyroscope. A number of different waveforms have been used to obtain analog serrodyne phase modulation including sawtooth, sinusoidal, and triangular as follows.

3.2.1. *Sawtooth Wave*

As shown in Figure 3.10, a phase modulator in a gyroscope driven by a sawtooth waveform provides a constant differential phase shift during a portion of the driving waveform period, which can be used to cancel the rotation induced phase shift The generation of a sawtooth waveform requires a phase modulator with a large frequency bandwidth to accommodate the fast reset that occurs once every cycle of the modulation waveform. For this reason electro-optic phase modulators made with a $LiNbO_3$ channel waveguide are used. In most cases the modulation amplitude ϕ_m is set to be 2π rad and the frequency f_m (or the period T) of the sawtooth waveform is adjusted to counteract the rotation-induced differential phase shift. In this case, the differential phase shift generated by the phase modulation during the time period $T - \tau$ is $\Delta\phi(t) = 2\pi f_m \tau$, and during the rest of the time near the reset of 2π is $2\pi f_m \tau - 2\pi$. Therefore when implemented in a closed-loop gyroscope, where the net differential phase shift is maintained at zero, the output of the gyroscope is the phase modulation frequency f_m, which is related to the rotation rate of the gyroscope as

$$f_m = (D/n\lambda)\Omega \tag{3.6}$$

which is the same as in the case of frequency shifting as in equation (3.5). One important note to mention is that the signal during the time period τ at each reset of the waveform by 2π rad can be used to calibrate and maintain the phase modulation amplitude at 2π with high precision.

Unlike the frequency shifter case, this approach requires only one phase modulator since the sawtooth waveform phase modulation (serrodyne frequency shifter) is equivalent to a baseband frequency shifter. For a rotation rate such that $T = \tau$, there will be no differential phase shift even though the phase modulator is operating, as can be understood with Figure 3.10. In this case the operating point of the gyroscope is translated by 2π from the zero phase difference in Figure 3.11. One of the important issues of the serrodyne phase modulation approach with a sawtooth waveform is the finite flyback time that introduces errors in the scale factor of the gyroscope. Practical implementation with sufficiently fast flyback is not trivial but has been demonstrated.

3.2.2. *Gated Phase Modulation Approach*

As we have seen, the saw tooth waveform serrodyne approach requires a phase modulator with a very wide frequency bandwidth and cannot be implemented in an all-fiber-optic gyroscope using a fiber-optic phase modulator with a very limited frequency bandwidth. Since the all-fiber gyro configuration has important advantages over the hybrid configuration (which uses a fiber sensing loop and integrated optic components) of low optical loss and simplicity of construction, it is important to investigate the possibility of building an all-fiber gyro with extended dynamic range while maintaining a high sensitivity of rotation measurement. The fundamental limitation of a fiber-optic phase modulator (a short section of a fiber wrapped around a piezoelectric cylinder under low tension) is that it can be driven effectively only with the sinusoidal modulation waveform, since it generally cannot support complex waveforms that consist of many harmonic-frequency components. The reason for this is the mechanical resonances of the piezoelectric cylinder that result in different amplitude and phase response to the harmonic contents of an arbitrary modulation waveform. In principle, however, an arbitrary phase-modulation waveform can be generated by supplying the individual Fourier harmonic components of the waveform. This can, however, be excessively complex for a practical implementation.

The simplest approximation to the sawtooth waveform is a waveform containing only one frequency component; namely, a sinusoidal waveform with a fixed modulation frequency and adjustable modulation amplitude [10]. As described in Section 2, a sinusoidal phase modulation applied to a

gyroscope produces a sinusoidal phase difference modulation. Contrary to the sawtooth waveform, the entire waveform of a sinusoidal differential phase modulation cannot be used to cancel the rotation induced phase shift when a constant rotation rate is applied to the gyroscope. However, if the gyroscope signal is turned off during every half cycle of the modulation waveform, the time-averaged differential phase shift produced by the remaining differential phase modulation can directly be used to null the rotation-induced phase shift. This process is very similar to the rectification of an ac electrical signal to produce a dc signal on the time average. The magnitude of time averaged differential phase shift is proportional to the phase modulation amplitude.

Figure 3.16 shows the schematic of a gated phase modulation gyroscope, where the phase modulator receives a dynamic bias modulation at frequency f_b with a fixed modulation amplitude, and the feedback phase modulation at frequency f_m with adjustable modulation amplitude. The electronic gate operates at 50% duty cycle in synchrony with the feedback phase modulation. The phase sensitive detector (PSD) monitors the photodetector current at the bias phase modulation frequency f_b, which is maintained at zero through an electronic servo loop that controls the amplitude of the feedback phase modulation. In order to get a sufficient time average during each half-cycle of the sinusoidal phase modulation for the feedback, f_m should be much smaller than the bias modulation frequency f_b, yet large enough to accommodate a fast change of rotation rates. During 50% of the time the rotation-induced gyro signal is canceled on the time average by the feedback phase modulation, and for the rest of the time a zero signal is simulated by turning the gyro signal off.

The scale factor of this approach with single sinusoidal phase modulation is not strictly linear even though it is monotonic. In order to improve the linearity of the scale factor, a next order approximation to the

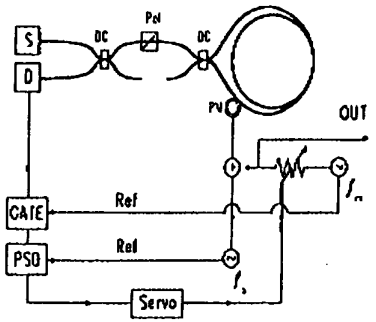

Fig. 3.16. Schematic of a closed-loop gyro using gated phase modulation.

sawtooth waveform can be made by introducing the second harmonic of the original phase modulation signal with proper relative phase and amplitude relationship [11], as shown in Figure 3.17. One can see that a relatively flat region in the differential phase modulation is achieved similar to the case of a sawtooth waveform. By choosing the proper portion of the flat region of the waveform, as shown in Figure 3.18, a great improvement of the linearity of the scale factor is achieved. A critical control of the relative phase and amplitude of the first and second harmonic signals should be maintained for a stable scale factor.

The major drawback of the gated phase modulation approach is that the rotation rate output is the amplitude of the phase modulation, which is typically difficult to measure with high accuracy. One of the reasons for this is that the response of the piezoelectric cylinder and an applied voltage is a function of environmental parameters, especially the temperature. Another reason is the difficulty of measuring the voltage of an ac signal with high precision with available electronics. If, however, the piezoelectric modulator can be stabilized independent of the gyro output, this approach can provide a scale factor independent of the source wavelength, since both the Sagnac phase shift and the coefficient of the

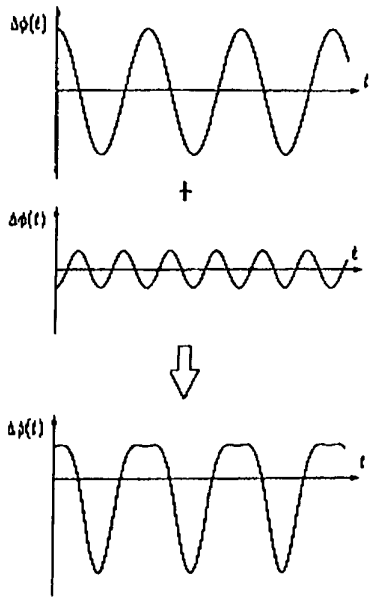

Fig. 3.17. Generation of differential phase modulation waveforms with almost a flat top for the use in the gated phase modulation signal processing.

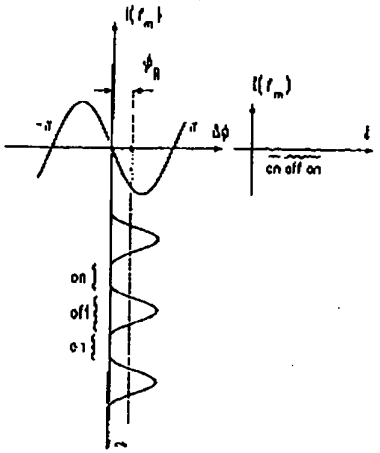

Fig. 3.18. The differential phase modulation waveform shown in Figure 3.17 is used to cancel the Sagnac phase shift ϕ_R with the help of an electronic gate.

phase modulation amplitude with respect to the applied voltage have the same source wavelength dependent $(1/\lambda)$ This could be a very important aspect of the phase modulation closed-loop approach, although there has not been a practical method of stabilizing a piezoelectric phase modulator.

3.2.3. *Asymmetric Triangular Waveform*

A relatively new approach to a serrodyne phase modulation for gyroscopes uses a triangular waveform whose symmetry in time becomes the rotation rate output, eliminating the difficulty encountered when the rotation output is in the form of a voltage, as described for the gated phase modulation approach. As described in Chapter 5 in detail, this approach uses a principle similar to that of the sawtooth waveform, but with phase ramps having two different slopes as shown in Figure 3.19(a), introducing a number of interesting and improved features [12]. The operating point of the gyroscope on the basic interferometer response curve is made to alternate between two symmetric points (for example, at $\Delta\phi = \pm N\pi$, where the detector current at the first harmonic of the bias modulation frequency is zero) instead of the being held at zero net differential phase shift, thus preserving reciprocity on the time average. As in the other closed-loop approaches this also uses an additional phase modulation for dynamic biasing, at much higher frequency than the one used for the closed loop operation.

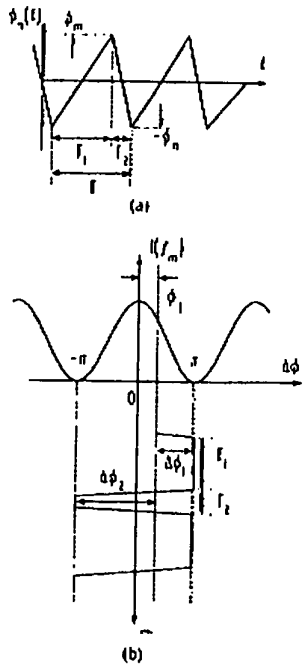

Fig. 3.19. (a) Asymmetric dual slope phase ramp. (b) Cancelation of Sagnac phase shift by using the dual slope phase ramp when the two operating points are $\pm\pi$.

The closed loop is formed such that during the time period T_1 the operating point is maintained at $\Delta\phi = +N\pi$, and for the rest of the modulation period T it is maintained at $-N\pi$, as shown in Figure 3.19(b) for $N = 1$. For a time period of τ near each turning point of the phase modulation waveform, the gyro output signal is not utilized, and only the portions of the differential phase modulation waveform that are constant in time are useful for the signal processing. If the modulation amplitude is ϕ_m, the differential phase shifts induced for the two time periods become (see Figure 3.19(b)) $\Delta\phi_1 = 2\phi_m\tau/T_1$ and $\Delta\phi_2 = -2\phi_m\tau/T_2$. With rotation-induced phase shift ϕ_R and with the closed loop operating, a simple calculation leads to

$$\phi_R = -1/2(\Delta\phi_1 + \Delta\phi_2) = -\phi_m\tau(1/T_1 - 1/T_2) = \phi_m\tau(T_1 - T_2)/T_1T_2$$
$$= \pi(T_1 - T_2)/(T_1 + T_2) \qquad (3.7)$$

Therefore, by measuring the periods of time for the up ramp and the down ramp, one can easily calculate the rotation rate with the help of equation

(3.7) and the scale factor of the gyroscope. Since the output of the gyroscope is in the form of time intervals that can be measured with high accuracy by conventional techniques, this approach eliminates the difficulty associated with the amplitude measurement for the gated phase modulation technique described in the previous section. One can notice that the phase modulation waveform in Figure 3.19(a) is basically the combination of two sawtooth waveforms with different ramping slopes and opposite signs. This point of view can also be seen from equation (3.7), where the nonreciprocal phase shift induced by the phase modulator is the sum of the phase shifts of two of the serrodyne frequency shifters described in Section 3.2.1, with opposite signs and corresponding magnitudes. Instead of having zero frequency for the sawtooth phase modulation in the case of a zero rotation rate, this approach utilizes the $\pm\pi$ differential phase shift that produces zero phase shift on the average.

A few important features of this approach are evident from equation (3.7). The measurement of rotation induced differential phase shift ϕ_R does not depend on the phase modulation amplitude and sensing loop transit time (or refractive index of the fiber) $\phi_m\tau$, very different from the ordinary serrodyne approach using a sawtooth waveform. Since this stabilization of the phase modulation amplitude is not a trivial task, this feature is an important advantage of this approach compared to others. When the rotation-induced differential phase shift is π, the waveform becomes the same as the sawtooth waveform. Beyond that rotation rate, the operating points have to be shifted to other appropriate points; for example, 0 and 2π instead of $\pm\pi$. Another important point is that the scale factor of this approach is independent of the refractive index of the fiber. The asymmetric triangular phase modulation waveform can easily be generated by an electro-optic modulator. When one wishes to use a fiber-optic phase modulator, however, the modulation frequency is limited to very low values to avoid interference with the mechanical resonance of the piezoelectric cylinder, requiring a large phase modulation amplitude. This requires a relatively large applied voltage to the phase modulator. Also, longer lengths of fiber are needed for the phase modulator and the sensing loop. An electro-optic phase modulator would be necessary for a gyroscope with short fiber coil.

3.3. Digital Serrodyne Phase Modulation

An important variation of serrodyne phase modulation applied to fiber gyroscopes is the use of a digital phase ramp [13, 14] as shown in Figure

3.20 and described in detail in Chapter 6. Instead of an analog phase ramp as shown in Figure 3.10, a series of phase steps with a small amplitude and a duration equal to the loop transit time τ is used, which produces basically the same type of differential phase shift between the counter-propagating waves as for the analog phase ramp. The only difference between the analog and the staircase phase modulation in a gyroscope is the transient behavior between the phase steps. Even though the digital phase ramp cannot be thought of as a general purpose frequency shifter, it is perfectly suitable for fiber gyroscopes using a Sagnac interferometer where only the differential phase shift matters between the two waves passing through the phase modulator with time difference of τ.

The modulation amplitude of the digital phase ramp can also be controlled to be kept at 2π rad, using the gyro signal during the phase reset of 2π, as in sawtooth waveform phase modulation. Coupled with a square wave bias modulation as described in Figure 3.8, synchronized with the digital phase ramp, a very convenient monitor signal for the deviation of the phase modulation amplitude from 2π can be obtained with this approach. This leads to double closed-loop operation of the gyroscope: one for cancelation of the rotation-induced differential phase shift, and another for maintaining the phase modulation amplitude at 2π.

This approach allows a very simple digital signal processing, and with the availability of high-speed electro-optic phase modulators, it is gaining popularity among the fiber gyroscope community. The change of refractive index of the fiber in the sensing loop, and thus τ, does not affect the scale factor of the gyroscope with this approach since it simply produces a timing error for the phase steps, which furthermore can be eliminated by

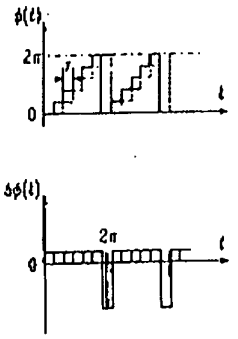

Fig. 3.20. The waveforms of a digital serrodyne phase modulation ($\phi(t)$) and that of the differential phase modulation ($\Delta\phi(t)$).

using an electronic gate that selects only a proper portion of the gyro signal between the staircase transitions. One of the major difficulties with this approach is with a fiber gyro having a relatively short fiber sensing coil and thus a small τ, since the useful signal portion becomes small, leading to problems with the response time and the synchronization of the phase modulator and its driving electronics along with the detection electronics.

The size of the phase step required is determined by the amount of optical noise (for example, shot noise) within the initial detection bandwidth, which is normally a few tens of MHz, making it acceptable to use the relatively large phase steps characteristic of conventional digital electronics.

3.4. Other Approaches

Thee have been a number of other approaches to closed-loop gyroscopes, including the use of the magneto-optic effect for the generation of nonreciprocal phase shift as well as the use of the interference of the harmonic waves of the phase modulation to generate a signal at the first harmonic of the bias phase modulation frequency, which cancels the signal generated by the rotation. Most of these approaches have more difficulties in practical implementation than the schemes described previously and are not the subject of extensive research at the present time.

4. OPEN-LOOP APPROACHES

As described in Section 1, open-loop approaches do not use a nonreciprocal phase shifter but require quadrature phase information; e.g., values of sine and cosine of the differential phase shift between the two counterpropagating waves in the sensing coil. Once the quadrature phase information is achieved, the phase difference $\Delta\phi$ can be measured without ambiguity (although the 2π ambiguity still exists) and without a loss of sensitivity. Therefore the key to the open-loop approach is to obtain the quadrature phase information without loosing the reciprocity of the optical paths for the counterpropagating waves.

There have been a number of techniques for this purpose, including the use of a 3×3 coupler [15], which unfortunately does not provide the reciprocity needed for the gyroscope. The most popular technique involves the sinusoidal differential phase modulation that results in the output detector current expressed in equation (3.3). The detector current contains

signals proportional to $\cos(\phi_R)$ at the even harmonics of the phase modulation frequency and $\sin(\phi_R)$ at odd harmonics of the modulation frequency. A straightforward method is to measure the magnitude of the odd and even harmonic components from the detector current and, by taking the ratio of the two values numerically, get the rotation-induced differential phase shift [16] as described in equation (3.4). This approach, however, is difficult to implement if one wants high sensitivity and stability, due to difficulties in measuring the amplitude of ac signals with great accuracy, as described for closed-loop gyroscopes, especially when two separate measurements are involved for signals at two different frequencies.

Another approach that may be more practical in terms of electronic implementation is to apply electronic signal processing to the detector output from a phase modulated gyroscope, which converts the optical phase difference between the counterpropagating waves into a phase shift of a low-frequency sinusoidal electronic signal. The electronic phase shift can be directly measured by using conventional time-interval counters or phase meters. In effect, this approach produces a gyro output that is the same as for a heterodyne interferometer, without using frequency shifters, and it is often called the *synthetic heterodyne method*. The generation of a sinusoidal electronic signal (phasor) that contains the optical phase difference information in its phase is done by translating signals that are proportional to $\sin\phi_R$ and $\cos\phi_R$, originally at odd and even harmonics of the phase modulation frequency, to the same frequency, thereby forming a phasor whose phase is equal to the optical phase difference ϕ_R. This is accomplished by modulating the detector current at the phase modulation frequency, thus producing sidebands of the original frequency components, resulting in the addition of even and odd harmonic components at the same frequency. In this case the amplitudes of the even and odd components being combined should be equal and the electronic phase difference between them should be $\pi/2$. That is,

$$\cos(\Delta\phi_R)\cos(\omega t) \pm \sin(\Delta\phi_R)\sin(\omega t) = \cos(\omega t \mp \Delta\phi_R) \qquad (3.8)$$

The resulting phasor signal has a constant amplitude independent of the rotation rate. The measurement of electronic phase shift is typically performed by comparing the zero crossings of two sinusoidal electronic signals using a time interval counter, so that the digital output does not depend on the intensity of the source or the gain parameters of the processing electronics, as in the case of closed-loop approaches. One of the major difficulties of this approach lies in the stable measurement of

the time interval between the zero crossings of two sinusoidal waveforms, which comes from the limitations of available electronics. The other issue is the need for the stabilization of the phase modulation amplitude since that affects the linearity of the scale factor to the first order.

More recently, a significant modification was introduced to the synthetic heterodyne open-loop approach that overcomes most of the problems associated with the existing signal processing. This approach uses a digital electronic phase-locked loop, eliminating most of the analog signal processing that imposes serious limitations on the stability of the rotation rate measurement. This approach involves multiplication of the detector current from a phase-modulated gyroscope by a digitally generated square waveform whose dc value is maintained at zero level by a feedback servo loop.

4.1. Synthetic Heterodyne

As described in Section 2, the detector output current from a phase modulated gyroscope contains harmonic frequency components of the phase modulation frequency whose magnitudes are proportional to $\sin(\phi_R)$ for odd harmonics and $\cos(\phi_R)$ for even harmonics. Even though one can measure the amplitude of the signals at odd and even harmonics separately and use them to calculate the rotation induced differential phase shift ϕ_R, it is not straightforward to perform the process with high accuracy and stability. The synthetic heterodyne approach transforms the information on ϕ_R, which is imbedded in the amplitudes of the harmonic signals, into the phase of a low-frequency electronic signal that can be measured with high accuracy using conventional counters [17, 18].

The addition of even and odd harmonic signals at a single frequency is achieved by amplitude modulation of the detector current with a simple 1×2 electronic switch operated at the phase modulation frequency f_m as shown in Figure 3.21. This produces sideband signals from each of the original frequency components that overlap adjacent frequency components. Therefore, the signals at each harmonic frequency Nf_m contain signals that are proportional to $\sin(\phi_R)$ and $\cos(\phi_R)$. The dc component of the detector current is eliminated before it goes to the switch, since it contains a signal that is irrelevant to the rotation rate, as can be seen from equation (3.3). Figure 3.22 shows the amplitude modulation signal waveforms and their timing for the two output channels in the schematic Figure 3.21. At the switch outputs, one harmonic frequency is selected for the phasor, by means of bandpass filters. In order to avoid possible interfer-

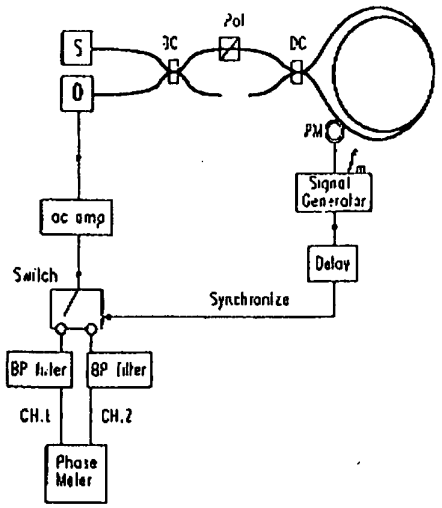

Fig. 3.21. Schematic of the open-loop two channel synthetic heterodyne gyroscope.

ence from the amplitude modulation signal, the signal at frequency $2f_m$ is preferably selected as the phasor. When the phase modulation amplitude is such that

$$J_2(\phi_m) = (8/\pi) \sum_{n=1}^{\infty} (-1)^n J_{2n-1}(\phi_m)/(2n-3)(2n+1) \equiv K = \text{constant} \tag{3.9}$$

then the bandpass filter outputs at frequency $2f_m$ from both channels have the same maximum amplitude providing a linear scale factor. In this case, the bandpass filter outputs I_1 and I_2 from the two channels become

$$\begin{aligned} I_1 &= (I_0 K/2)\cos(2\omega_m t + \phi_R) \\ I_2 &= (I_0 K/2)\cos(2\omega_m t - \phi_R) \end{aligned} \tag{3.10}$$

The measurement of the phase difference of the two signals from the two channels yields $2\phi_R$. The value of ϕ_m that satisfies equation (3.9) is about 2.8 rad.

The use of the two sinusoidal signals generated from a single detector current for the measurement of the phase difference eliminates common phase errors induced by various electronic components such as phase modulator, amplifier, and switch. Deviation of the phase modulation

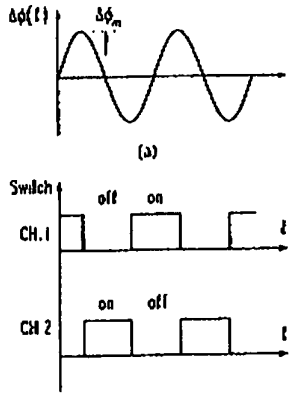

Fig. 3.22. Timing of the electronic amplitude modulation waveform for the two channels with respect to the differential phase modulation for the synthetic heterodyne gyroscope.

amplitude from the desired value, and the difference of the phase response of the two bandpass filters, cause first-order errors in rotation rate measurement. Along with the errors in the time-interval counting for the zero crossings of the two sinusoidal waveforms, these error sources are the limiting factors for the synthetic heterodyne approach.

This approach provides effectively infinite dynamic range for the rotation rate without requiring wide dynamic range for any of the electronic or optical components except for the time-interval counter, which inherently has a wide-enough dynamic range.

4.2. Digital Phase Locked Loop

In order to avoid problems with the synthetic heterodyne approach associated with the stability of analog electronic elements described in the previous section, a new approach has been demonstrated using mainly digital electronics and also a single electronic signal channel instead of two [19]. The schematic of the gyroscope, as shown in Figure 3.23, has an open-loop optical circuit but a closed-loop digital electronic circuit for the measurement of optical phase shift. Instead of the square wave used for the synthetic heterodyne approach, this approach utilizes a train of square pulses with adjustable pulse spacing in response to the rotation-induced optical phase difference (see Figure 3.24). The dc component in the output from the mixer, which is a simple switch in this case, is selected using a

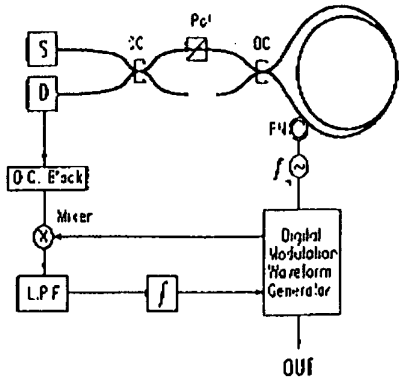

Fig. 3.23. Schematic of the open-loop gyroscope with digital phase locked loop signal processing. *LPF*: low pass filter.

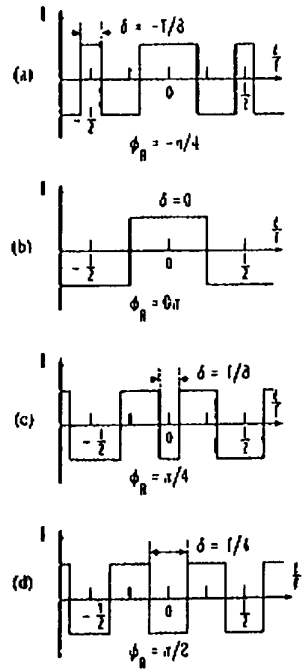

Fig. 3.24. Digital waveforms for the digital phase locked loop gyroscope for several values of rotation induced Sagnac phase shift.

low-pass filter and is fed to the digital modulation waveform generator, which in turn modifies the digital pulse spacing δ in the direction to bring the dc feedback signal to zero. The spacing δ between the pulses then reflects the rotation-induced optical phase shift. Its value is known from the digital electronics, so that a separate measurement of this pulse spacing is not needed.

The underlying principle of this approach can be understood by examining the special waveform shown in Figure 3.24 for several values of ϕ_R when the electronic loop is closed. The modulation waveform is a periodic function with period $T = 1/f_m$, which is the same as the phase modulation period. The width of the square pulses is $T/4$, and these pulses move symmetrically with respect to $t/T = 0$ in the figure when the pulse spacing δ varies in response to the rotation rate input. One can notice that the modulation waveform becomes a square waveform at frequency f_m with 50% duty cycle when δ is zero, and it becomes a square waveform at frequency $2f_m$ when $\delta = T/4$, which corresponds to a rotation-induced differential phase shift of $\pi/2$. In other words, the amplitude modulation waveform contains only the odd (even) harmonics of the phase modulation frequency when the original detector current contains only the even (odd) harmonics of the phase modulation frequency, keeping the dc component in the detector current at zero value.

At other rotation rates, the amplitude modulation signal contains both the even and odd harmonics of the phase modulation frequency. In this case, the dc component, produced by the multiplication of the odd harmonics in the detector current with those in the amplitude modulation signal, has the same magnitude with the opposite sign compared to that produced by the multiplication of even harmonics in the two signals. Just as the odd and even harmonic contents in the detector current vary with the rotation rate input, the even and odd harmonic contents in the amplitude modulation signal vary with the time interval δ of the digital square pulses. From the preceding observations, it is not difficult to realize that the special mirror image waveform depicted in Figure 3.24 produces harmonic contents similar to the output from an open-loop gyroscope and can be used to transform the rotation-induced differential phase shift to the time interval δ between the square pulses when the electronic loop is closed and that δ can be easily determined a priori from the digital electronic signal generator. Another way of looking at this approach is that it is a modified form of a synthetic heterodyne approach with single electronic channel and digital phase locked loop for the time interval measurement.

A detailed calculation leads to the relationship between the differential phase shift $\Delta\phi_R$ and the time interval δ as

$$\phi_R = \tan^{-1}[S_\epsilon(2\pi\delta/T)/C_\epsilon(2\pi\delta/T)] \tag{3.11}$$

$$S_\epsilon(2\pi\delta/T) = \sum_{n=1}^{\infty} \left[J_{2(2n-1)}(\phi_m)/(2n-1)\right] \sin[(2n-1)(2\pi\delta/T)] \tag{3.12}$$

$$C_\epsilon(2\pi\delta/T) = \sum_{n=1}^{\infty} [J_{2n-1}(\phi_m)/2n-1] \times \{\text{sign}[\cos(\pi\delta/T)]\cos[(2n-1)(\pi\delta/T)] + (-1)^n \text{sign}[\sin(\pi\delta/T)]\sin[(2n-1)(\pi\delta/T)]\} \tag{3.13}$$

$$\text{sign}(x) = \{1 \text{ if } x > 0, \quad -1 \text{ if } x < 0\} \tag{3.14}$$

Figure 3.25 shows the relationship between the pulse spacing δ and the differential phase shift ϕ_R for several values of the phase modulation amplitude ϕ_m. As can be seen, the linearity of the response depends on the phase modulation amplitude, and the best linearity is obtained at $\phi_m = 2.77$ rad, where the maximum deviation from a perfect linearity is 7 mrad, which can easily be corrected with a microprocessor. This also means the phase modulation amplitude has to be stabilized to an accuracy required by the gyroscope application as in the case of the synthetic heterodyne open-loop approach and also as in the serrodyne closed-loop

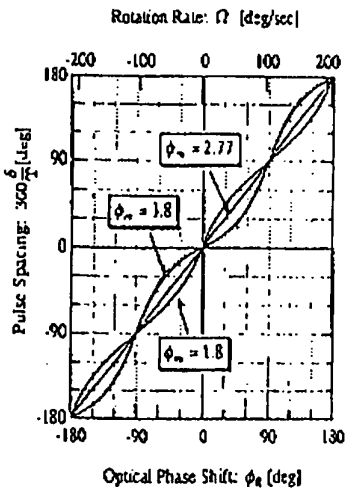

Fig. 3.25. Scale factor of the digital phase locked loop gyroscope for several values of the phase modulation amplitude.

approaches. This could be accomplished by implementing a second digital signal process similar to the main phase locked loop for the gyroscope, resulting in dual electronic closed-loop operation as in the case of the digital serrodyne approach described in Section 3.3. The number of digital steps for the pulse spacing δ required for the resolution of the gyroscope need not be large if an integrator for the error signal is employed in the feedback circuit, which is basically the same as for the digital serrodyne approach. The details of practical implementation are still being developed.

This approach eliminates most of the basic problems encountered with synthetic heterodyne systems, described in the previous section, arising from the balancing of two separate electronic channels, since it uses only one signal channel and digital electronics. This approach seems to have the best potential to date for an open-loop fiber-optic gyroscope.

4.3. Other Approaches

A number of different open-loop approaches investigated using phase modulation single-sideband detection [20] and true heterodyne detection with an acousto-optic frequency shifter with reciprocal operation [21] produce the same nature of output and share the same difficulties as the synthetic heterodyne gyroscope but with more complicated optical and electronic circuits. A passive quadrature detection scheme, using two orthogonal polarization modes in the sensing fiber coil [22], has been proposed, but it does not provide the reciprocity that may be needed for high-accuracy gyroscope applications.

One open-loop approach that should be mentioned is the simple phase modulated open-loop gyro with its first harmonic signal as the output, as described in Section 2, that has only a limited dynamic range. This can be a very practical way of building a gyro whose application does not require a wide dynamic range, in which case the scale factor stabilization is done by a straightforward stabilization of optical and electronic parameters. One of the options for increasing the dynamic range is to use two wavelengths for the source [23].

5. CONCLUSION

As described in this chapter, there are a number of different approaches to fiber gyroscopes with a wide linear dynamic range. The choice of a

particular approach should be based on the performance requirements, availability of various optical and electronic components at a given time and place, and other factors such as cost. It seems that some of the approaches described previously may not survive in the future, but a few will become standard for applications with different requirements. Some of the techniques have been engineered far more diligently than others, but it seems important to pursue some other approaches a little further since different techniques have their own merits. For this reason, further research on the comparative features for various approaches to fiber optic gyroscopes is desirable.

REFERENCES

[1] Ulrich, R. (1980). "Fiber optical rotation sensing with low drift," *Optics Letters* 5(5), 173–175.

[2] Bergh, R. A., Lefevre, H. C., and Shaw, H. J. (1981). "All single-mode fiber-optic gyroscope with long-term stability," *Optics Letters* 6(10), 502–504.

[3] Lefevre, H. C., Bergh, R. A., and Shaw, H. J. (1982). "All-fiber gyroscope with inertial-navigation short-term sensitivity," *Optics Letters* 7(9), 454–456.

[4] Cahill, R. F., and Udd, E. (1979). "Phase-nulling fiber-optics laser gyro," *Optics Letters* 4(3), 93–95.

[5] Davis, J. L., and Ezekiel, S. (1982) "Closed loop, low-noise, fiber-optic rotation sensor," *Optics Letters* 6(10), 505–507.

[6] Auch, W. (1986) "Fiber optic gyro—a device for laboratory use only?" Fiber Optic Gyros: 10th Anniversary Conference (Cambridge, Mass., 24–26 Sept. 1986), *Proc. SPIE* 719, 28–34.

[7] Kim, B. Y., Blake, J. N., Engan, H. E., and Shaw, H. J. (1986) "All-fiber acousto-optic frequency shifter," *Optics Letters* 11(6), 389–391.

[8] Enrero, A., and Schiffner, G. (1985). "Closed-loop fiber-optic gyroscope with sawtooth phase-modulated feedback," *Optics Letters* 10(6), 300–302.

[9] Kay, C. J. (1985). "Serrodyne modulator a fibre-optic gyroscope," *IEE Proc Pt. J-Optoelectron* (GB), 132(5), 259–264.

[10] Kim, B. Y., and Shaw, H. J. (1984). "Gated phase-modulation feedback approach to fiber-optic gyroscopes," *Optics Letters* 9(6), 263–265.

[11] Kim, B. Y., and Shaw, H. J. (1984). "Gated phase-modulation approach to fiber-optic gyroscope with linearized scale factor," *Optics Letters* 9(8), 375–377

[12] Bergh, R. A. (1989). "Dual-ramp closed-loop fiber optic gyroscope," Fiber Optic and Laser Sensors VII Conference (Boston, 5–7 Sept. 1989), *Proc. SPIE* 1169, paper 1169-71.

[13] Lefevre, H. C., Graindorge, P., Arditty, H. J., Vatoux, S., and Papuchon, M. (1985). "Double closed-loop hybrid gyroscope using digital phase ramp,"

3rd Intl. Conf. Optical Fiber Sensors (OFS'85) (San Diego, 13–14 Feb. 1985), post deadline paper PDS 7.1–7.8.

[14] Arditty, H. J., Graindorge, P., Lefevre, H. C., Martin, P., and Morisse, J. (1989). "Fiber optic gyroscope with all-digital closed-loop processing," *Optical Fiber Sensors*, Springer Proceedings in Physics 44. Springer Verlag, Berlin, pp. 131–136.

[15] Sheem, S. K. (1980). "Fiber optic gyroscope with (3 × 3) directional coupler," *Applied Physics Letters* 37(10), 869–871.

[16] Bohm, K., Marten, P., Weidel, E., and Petermann, K. (1983). "Direct rotation rate detection with a fiber optic gyro by using a digital data processing," *Electron Letters* 19(23), 997–999.

[17] Kim, B. Y., and Shaw, H. J. (1984). "Phase-reading all-fiber-optic gyroscope," *Optics Letters* 9(8), 378–380.

[18] Kersey, A. D., Lewin, A. C., and Jackson, D. A. (1984). "Pseudo-heterodyne detection scheme for the fiber gyro," *Electron Letters* 20(9), 368–370.

[19] Toyama, K., Fesler, K. A., Kim, B. Y., and Shaw, H. J. (1991). "Digital integrating fiber-optic gyroscope with electronic phase tracking," *Optics Letters* 16(15), 1207–1209.

[20] Eberhard, D., and Voges, E. (1984). "Fiber gyroscope with phase-modulated single-sideband detection," *Optics Letters* 9(1), 22–24.

[21] Culshaw, B., and Giles, I. P. (1982). "Frequency modulated heterodyne optical fiber sagnac interferometer," *IEEE J. Quantum Electrons* QE-18(4), 690–693.

[22] Jackson, D. A., Kersey, A. D., and Lewin, A. C. (1984). "Fiber gyroscope with passive quadrature detection," *Electron Letters* 20(10), 399–401.

[23] Kersey, A. D., Dandridge, A., and Burns, W. K. (1986). "Two-wavelength fiber gyroscope with wide dynamic range," *Electrons Letters* 22(18), 935–937.

Section II

DEVICES AND COMPONENTS